

# A Theoretical Study of the Aminolysis Reaction of Lysine 199 of Human Serum Albumin with Benzylpenicillin: Consequences for Immunochemistry of Penicillins

Natalia Díaz,<sup>†</sup> Dimas Suárez,<sup>‡,§</sup> Tomás L. Sordo,<sup>†</sup> and Kenneth M. Merz, Jr.<sup>\*‡</sup>

Contribution from the Departamento de Química Física y Analítica, Universidad de Oviedo, C/Julián Clavería 8, 33006 Oviedo, Asturias, Spain, and Department of Chemistry, Eberly College of Sciences, The Pennsylvania State University, 152 Davey Laboratory, University Park, Pennsylvania 16802-6300

Received February 6, 2001

**Abstract:** Herein, we present results of a computational study on benzylpenicillin attachment to Lys199 of human serum albumin via an aminolysis reaction. The internal geometry of the reactive part of the system was taken from previous work at the B3LYP/6-31+G\* level on the water-assisted aminolysis reaction of a penicillin model compound (Díaz, N.; Suárez, D.; Sordo, T. L. *J. Am. Chem. Soc.* **2000**, *122*, 6710–6719). The protein environment around Lys199, the 6-acylamino side chain, and the 2-methyl groups of benzylpenicillin were relaxed by carrying out geometry optimizations with a hybrid QM/MM method (PM3/AMBER). Two different mechanistic routes were explored: a one-step water-assisted process and a carboxylate and water-assisted route in which the  $\beta$ -lactam carboxylate and the ancillary water molecule mediate the proton transfer from the  $\epsilon$ -amino group of Lys199 to the  $\beta$ -lactam leaving N atom. The corresponding energy profiles in the protein combine the B3LYP/6-31+G\* and PM3 energies of the reactive subsystem (benzylpenicillin + Lys199 side chain + the ancillary water molecule) and semiempirical PM3 energies of the entire system evaluated with a “divide and conquer” linear-scaling method. It is observed that penicillin haptation to HSA can proceed through the water-assisted concerted mechanism which is calculated to have a high energy barrier of  $\sim 38$  kcal/mol, in agreement with the experimentally observed slow reaction kinetics.

## Introduction

Adverse reactions to penicillins and related  $\beta$ -lactam antibiotics is one of the main problems in drug allergy.<sup>1</sup> Some of the most dangerous clinical syndromes (for example, anaphylaxis or hemolytic anemia) involve the formation of immunoglobulin E or immunoglobulin G antibodies,<sup>2,3</sup> while other symptoms, such as exanthemas, can be connected to cellular events.<sup>4</sup> Classical immunochemical studies have shown that haptens (substances such as penicillins and other drugs with low molecular weight) can induce the formation of specific antibodies as a direct consequence of their chemical reactivity against plasma proteins.<sup>5</sup> The current understanding of drug hypersensitivity is based on this hapten hypothesis: (a) drugs bind covalently to plasma proteins to form protein–drug conjugates; (b) a specific site of this conjugate, the antigenic determinant, is then recognized by the immune system. Thus, production of protein–drug conjugates is central to the risk of penicillin

allergy, although other processes related to antigen presentation and antibody production are also involved.

The principal mode of conjugation of penicillins involves the formation of amide bonds through an aminolysis reaction with lysine groups of human serum albumin (HSA). The resulting adduct has an opened  $\beta$ -lactam ring (penicilloyl group), which has no antibacterial activity.<sup>6</sup> HSAs are the major soluble protein constituents of the circulatory system and are involved in the transport, distribution, and metabolism of many endogenous ligands (fatty acids, bilirubin, amino acids, metals, etc.) and numerous pharmaceuticals as well.<sup>7</sup> The tertiary structure of HSA is composed of three partially overlapping domains, domain I (residues 1–197), domain II (residues 189–385), and domain III (residues 381–585), which are characterized by a common motif of 10  $\alpha$ -helices.<sup>8,9</sup> Each domain is divided into two subdomains (A–B) so that the helices h1–h4 in subdomain A are homologous to h7–h10 in the corresponding subdomain B. The three-domain design of HSA provides a variety of binding sites, which can interact with a broad spectrum of compounds.<sup>8</sup> The formation of penicilloyl groups occurs at six specific lysine residues of HSA, which has a total of 59 lysine residues.<sup>10</sup> The primary site of penicilloyl coupling occurs at

\* To whom correspondence should be addressed. Phone: (814) 863 3623. Fax: (814) 863 8403. E-mail: merz@psu.edu.

<sup>†</sup> Universidad de Oviedo.

<sup>‡</sup> The Pennsylvania State University.

<sup>§</sup> On leave from Departamento de Química Física y Analítica, Universidad de Oviedo.

(1) Baldo, B. A.; Pham, N. H. *Chem. Res. Toxicol.* **1994**, *7*, 703–721.

(2) Blanca, M.; Vega, J. M.; García, J.; Miranda, A.; Carmona, M. J.; Juárez, C.; Terrados, S.; Fernández, J. *Clin. Exp. Allergy* **1994**, *24*, 407–415.

(3) Saxon, A.; Beall, G. N.; Rohr, A. S.; Adelman, D. C. *Ann. Intern. Med.* **1987**, *107*, 204–215.

(4) Padovan, E.; Bauer, T.; Tongio, M. M.; Kalbacher, H.; Weltzein, H. *Eur. J. Immunol.* **1997**, *27*, 1303–1307.

(5) Benjamini, E.; Coico, R.; Sunshine, G. *Immunology*, 4th ed.; Wiley-Liss: New York, 2000.

(6) Levine, B. B.; Ovary, Z. *J. Exp. Med.* **1961**, *114*, 875–904.

(7) Peters, T. *All about Albumin: Biochemistry, Genetics and Medical Applications*; Academic Press: San Diego, 1996.

(8) Carter, D. C.; Ho, J. X. *Adv. Protein Chem.* **1994**, *45*, 153–203.

(9) Sugio, S.; Mochizuki, S.; Noda, M.; Kashima, A. *Protein Eng.* **1999**, *12*, 439–446. PDB ID code 1AO6.

(10) (a) Yvon, M.; Anglade, P.; Val, J. M. *FEBS Lett.* **1988**, *239*, 237–240. (b) Yvon, M.; Anglade, P.; Val, J. M. *FEBS Lett.* **1989**, *247*, 273–278. (c) Yvon, M.; Anglade, P.; Val, J. M. *FEBS Lett.* **1990**, *263*, 237–240.

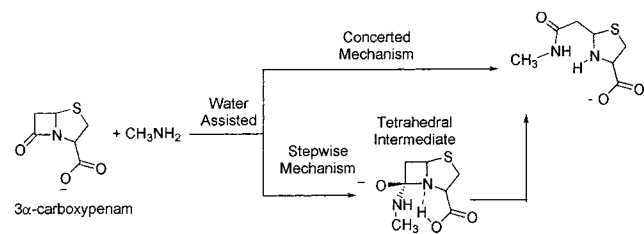
the  $\epsilon$ -amino group of Lys199,<sup>10a</sup> located strategically in the so-called IIA binding site of HSA, which noncovalently binds small, negatively charged hydrophobic molecules such as aspirin, *p*-nitrophenylacetate, triodobenzoic acid, etc.<sup>7,8</sup> Interestingly, the Lys199 residue can also act as a nucleophile against IIA ligands such as aspirin and trinitrobenzenesulfonate.<sup>11,12</sup>

Clearly, the overall protonation state of Lys199 will determine the reaction mechanisms of the aminolysis reaction with penicillins. The critical feature of the most likely mechanisms would require the  $\epsilon$ -amino group of the reactive lysine to be deprotonated in order to facilitate the nucleophilic attack toward electrophilic substrates. Interestingly, HSA modifications by the nonenzymatic reaction of glycosyl and arylating reagents have revealed the presence of unusually nucleophilic lysine residues, and, indeed, Lys199 is one of these.<sup>13</sup> This chemical behavior is consistent with an unusually low  $pK_a$  of  $\sim 8$  for Lys199, which implies the existence of a significant amount of the neutral form at physiological pHs. However, we also note that the  $pK_a$  of Lys199 has not been measured directly by either theoretical or experimental means.

Recently, we carried out restrained molecular dynamics (MD) simulations on HSA.<sup>14</sup> The influence that the charge state on Lys199 or the nearby Lys195 residue has on the structural and dynamical properties of the IIA binding site was addressed by studying the different possible protonation states. It was concluded that the average structure from the MD trajectory in which Lys195 and Lys199 were protonated and deprotonated, respectively, satisfactorily explains the residue–residue contacts observed in the X-ray structure,<sup>9</sup> in agreement with the proposed low  $pK_a$  value for Lys199. In the simulations, a stable first solvation sphere around the Lys199  $\epsilon$ -amino group containing  $\sim 2$  water molecules was also observed.

In previous work,<sup>15–19</sup> we performed a series of quantum chemical studies on the aminolysis of  $\beta$ -lactam compounds in order to obtain a sequence of models based on more detailed descriptions of this process. A B3LYP/6-31+G\* study predicted that the most favored mechanism in aqueous solution for the water-assisted aminolysis of a penicillin model compound, 3 $\alpha$ -carboxypenam (CP), is a concerted route, while a stepwise mechanism passing through a tetrahedral intermediate would be the most favored in the gas phase or in a low-polarity environment (see Scheme 1).<sup>18</sup> Interestingly, the carboxylate group of penicillins can exert a large kinetic influence, either enhancing the solute–solvent interactions along the concerted (water-assisted) reaction profile or acting as a proton shuttle in the stepwise (water and carboxylate-assisted) mechanism. This function of the carboxylate group as a proton shuttle resembles that observed in the hydrolysis reaction of aspirin, where the carboxylate group acts as a general base catalyst.<sup>20</sup> Taking into

## Scheme 1



account the X-ray structure and experimental data regarding the binding ability of the IIA binding site in HSA,<sup>8–10</sup> we have proposed that the most favorable mechanism for the aminolysis of penicillins and Lys199 in this protein environment could be analogous to the carboxylate and water-assisted mechanism found for the aminolysis of 3 $\alpha$ -carboxypenam.<sup>18</sup>

In the present work, we report a computational study on the water-assisted aminolysis reaction between benzylpenicillin (BP) and the Lys199 residue of HSA which takes into account the effect of water and the protein environment. The transition states and intermediate involved in the aminolysis reaction of 3 $\alpha$ -carboxypenam were employed to build the internal geometry of the reactive part of the HSA–BP complexes. A combined quantum mechanical (QM) method and a molecular mechanical (MM) method was used to relax, via energy minimization, the environmental water molecules, the protein residues surrounding the reactive lysine, the 6-acylamino side chain, and the 2-methyl groups of BP. The resultant structures were then employed to compute the energy profile in the protein for the water-assisted and carboxylate and water-assisted mechanisms. To this end, linear-scaling semiempirical calculations accounting for environmental effects were combined with density functional theory calculations on the reactive part of the system, which is not accurately described by semiempirical methods. Finally, the utility of the results for understanding the process of penicillin haptentation to HSA is discussed.

## Computational Methods

Different procedures based on a mixed QM/MM approach<sup>21,22</sup> have been developed to provide a fully flexible description of protein–substrate transition structures and complexes.<sup>23</sup> Although some ab initio QM/MM calculations of free energies and reaction paths have recently been reported,<sup>24</sup> most of the QM/MM applications have used semiempirical Hamiltonians for the key residues and substrate while the rest of the system was represented by a classical force field. However, for some reactive processes, semiempirical methods predict transition structures and intermediates which are quite inaccurate in terms of geometries and/or relative energies.<sup>25,26</sup> Unfortunately, we found that the geometry and relative energies of the critical points located on the PM3 or AM1 potential energy surfaces (PES) for the aminolysis reaction between CP and methylamine differ substantially from those obtained at the B3LYP/6-31+G\* level.

Figure 1 gives the most important critical points located along the reaction coordinate for the water-assisted aminolysis of 3 $\alpha$ -carboxypenam at the B3LYP/6-31+G\* level.<sup>18</sup> The two main TSs present a tight

(20) (a) Fersht, A. R.; Kirby, A. J. *J. Am. Chem. Soc.* **1967**, *89*, 4853–4856; (b) 4857–4863.

(21) Monard, G.; Merz, K. M., Jr. *Acc. Chem. Res.* **1999**, *32*, 904–911.

(22) Warshel, A.; Levitt, M. *J. Mol. Biol.* **1976**, *103*, 227–249.

(23) Turner, A.; Moliner, V.; Williams, I. H. *Phys. Chem. Chem. Phys.* **1999**, *1*, 1323–1331.

(24) (a) Bentzien, J.; Muller, R. P.; Florián, J.; Warshel, A. J. *Phys. Chem. B* **1998**, *102*, 2293–2301. (b) Liu, H.; Zhang, Y.; Yang, W. *J. Am. Chem. Soc.* **2000**, *122*, 6560–6570.

(25) Mullholand, A. J.; Richards, W. G. *Int. J. Quantum Chem.* **1994**, *51*, 161–172.

(26) Kuhn, B.; Kollman, P. A. *J. Am. Chem. Soc.* **2000**, *122*, 3909–3916.

(11) Gerig, J. T.; Katz, R. E.; Reinheimer, J. D.; Sullivan, G. R.; Roberts, J. D. *Org. Magn. Reson.* **1981**, *15*, 158–161.

(12) Kurono, Y.; Ichioka, K.; Ikeda, K. *J. Pharm. Sci.* **1983**, *72*, 432–435.

(13) (a) Gerig, J. T.; Reinheimer, J. D. *J. Am. Chem. Soc.* **1975**, *97*, 168–173. (b) Gerig, J. T.; Katz, R. E.; Reinheimer, J. D. *Biochim. Biophys. Acta* **1978**, *534*, 196–209.

(14) Díaz, N.; Suárez, D.; Sordo, T. L.; Merz, K. M., Jr. *J. Med. Chem.* **2001**, *44*, 250–260.

(15) Díaz, N.; Suárez, D.; Sordo, T. L. *Chem. Eur. J.* **1999**, *5*, 1045–1054.

(16) Díaz, N.; Suárez, D.; Sordo, T. L. *J. Org. Chem.* **1999**, *64*, 3281–3289.

(17) Díaz, N.; Suárez, D.; Sordo, T. L. *J. Org. Chem.* **1999**, *64*, 9144–9152.

(18) Díaz, N.; Suárez, D.; Sordo, T. L. *J. Am. Chem. Soc.* **2000**, *122*, 6710–6719.

(19) Díaz, N.; Suárez, D.; Sordo, T. L. *Eur. J. Org. Chem.* **2001**, 793–801.

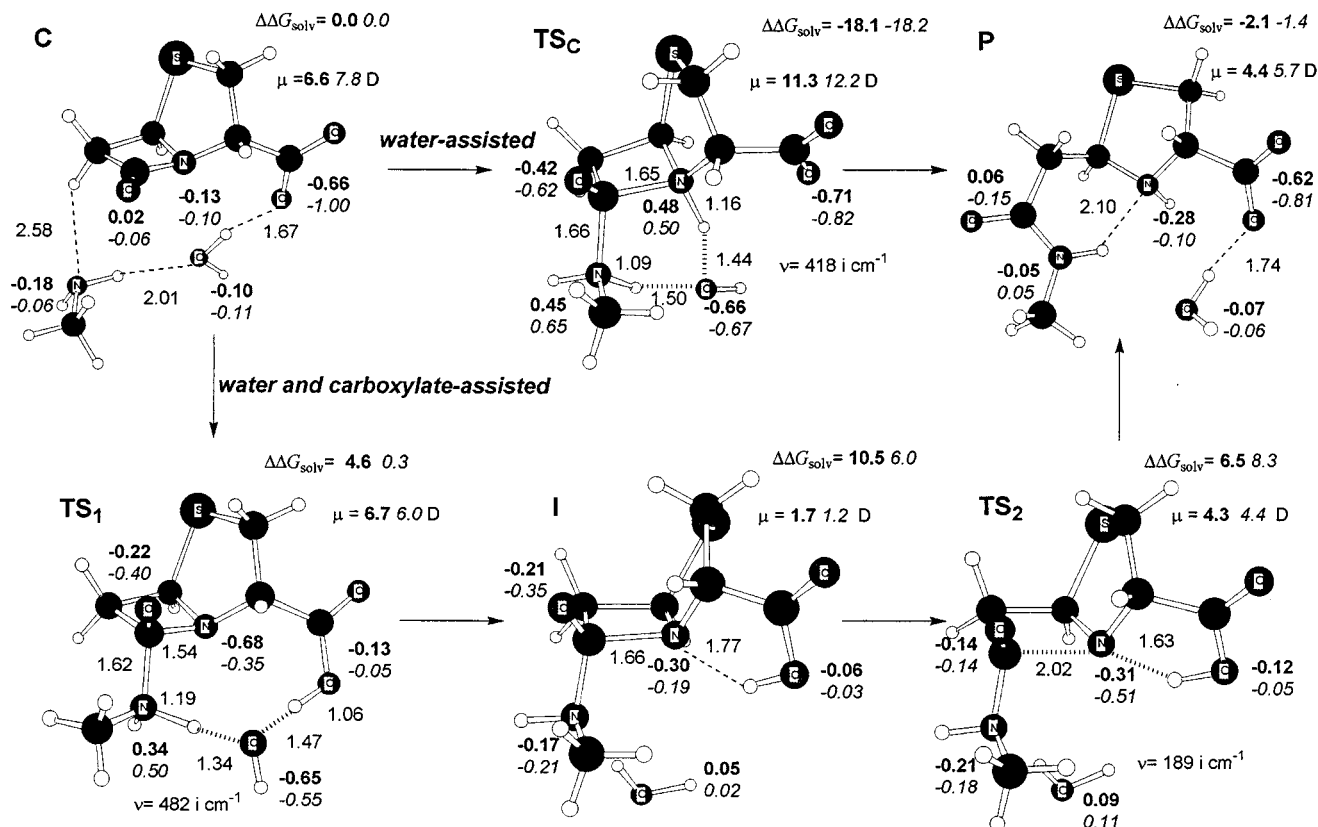


**Figure 1.** B3LYP/6-31+G\* optimized geometries for the structures involved in the aminolysis reaction of 3 $\alpha$ -carboxypenam (see ref 18). Distances in angstroms. Relative solvation energies (kcal/mol), dipole moments (debye), and EPS atomic charges for selected functional groups are given in bold (B3LYP/6-31+G\*) and italic (PM3) characters.

structure with the exocyclic C–N bond nearly formed ( $\sim 1.6$  Å) and with the endocyclic C–N bond barely cleaved ( $\sim 1.5$ – $1.7$  Å). These results are in consonance with other computational evidences suggesting that TSs are robust molecular entities whose essential structural features are invariant with respect to the nature of their environment.<sup>27</sup> Therefore, we docked the critical points of the CP + methylamine system<sup>18</sup> within the IIA binding site of HSA by performing QM/MM geometry optimizations in which the internal geometry of the reactive core (i.e., the  $\beta$ -lactam-thiazolidine part of BP, the amino group of Lys199, and the catalytic water molecule) was constrained and the rest of the system was relaxed.

**Construction of the Initial HSA–BP Template.** The starting point for this work was a snapshot produced from the MD simulation of the native form of the IIA binding site of HSA in which the Lys199 residue was neutral. Details of the simulation are described elsewhere.<sup>14</sup> This configuration was then subjected to geometry optimization, and, subsequently, a subsystem formed by all residues within a distance of 20 Å to the N $\zeta$ @Lys199 atom and the cap water molecules was chosen. Terminal *N*-methylamine or acetyl groups were placed at the C and N backbone atoms of those residues cleaved from the protein main chain by the truncation process. Cl<sup>−</sup> counterions were placed using LEAP<sup>28</sup> to neutralize the +6 charge of this HSA subsystem. All of the counterions were placed 20 Å beyond the N $\zeta$ @Lys199 atom. This molecular model of the native HSA (a pseudosphere containing  $\sim 5200$  atoms) includes nearly all of the residues of subdomain IIA of HSA as well as several residues from the rest of the remaining subdomains. Subsequently, the structure of a tetrahedral intermediate formed via the nucleophilic attack of the Lys199  $\epsilon$ -amino group toward BP was built by molecular modeling and docked manually into the IIA binding pocket so that the 6-acylamino side chain of BP was buried in the hydrophobic pocket of the IIA binding site. The resulting HSA–BP structure was divided into a QM region comprising the BP substrate,

the ancillary water molecule, and the side chain of Lys199, which was treated by the PM3 Hamiltonian (for a total of 59 atoms).<sup>29</sup> The rest of the protein atoms and water molecules were represented by the parm96 version of the AMBER force field.<sup>30</sup> The van der Waals parameters for the BP atoms were assigned the values of similar atom types in the AMBER force field. One hydrogen link atom was attached to the C $\beta$ @Lys199 atom to cap the exposed valence due to the C $\beta$ –C $\alpha$  bond crossing the QM/MM boundary.<sup>22</sup> To preserve integral charge for the AMBER region, the partial charges of the C $\alpha$  and H $\alpha$  atoms of Lys199 were changed to  $-0.028$  and  $0.143$ . In addition, a 15 Å active zone centered on the N $\zeta$ @Lys199 atom was defined, and only residues with at least half of their heavy atoms within this sphere as well as the cap water molecules were allowed to move during the PM3/AMBER minimizations ( $\sim 50\%$  of the system). The QM/MM partition and the active zone defined here were used in all of the subsequent PM3/AMBER calculations. The initial HSA–BP structure was then subjected to a short MD simulation of 2.0 ps followed by energy minimization in order to properly relax the protein–substrate contacts. Finally, the coordinates corresponding to the  $\beta$ -lactam-thiazolidine-carboxylate moiety of BP, the ancillary water molecule, and the C $\delta$ H<sub>2</sub>–N $\zeta$ H<sub>2</sub> moiety of Lys199 were deleted, and the resulting structure was used as an HSA–BP template.

**Construction of the HSA–BP Reactive Configurations.** Figure 2 sketches the computational approach followed in this work in order to obtain geometries and relative energies for different reactive configurations of the aminolysis reaction between BP and the Lys199 residue in HSA. As mentioned above, the internal geometry of the reactive part (i.e., the bicyclic nucleus of BP, the C $\delta$ –N $\zeta$ H<sub>2</sub> group from Lys199, and the ancillary water molecule; see Figure 2) was taken from our previous B3LYP/6-31+G\* gas-phase study.<sup>18</sup> We then docked the water-assisted TS (TS<sub>C</sub>) and the first TS of the carboxylate and water-assisted mechanism (TS<sub>1</sub>) within the HSA–BP template. The position

(27) Moliner, V.; Andrés, J.; Oliva, M.; Safont, V. S.; Tapia, O. *Theor. Chim. Acc.* **1999**, *101*, 228–233.

(28) Schafmeister, C.; Ross, W. S.; Romanovski, V. *LEAP*; University of California, San Francisco, 1995.

(29) Stewart, J. P. *J. Comput. Chem.* **1989**, *10*, 221–263.

(30) Cornell, W. D.; Cieplak, P.; Bayly, C. I.; Gould, I. R.; Merz, K. M., Jr.; Ferguson, D. M.; Spellmeyer, D. C.; Fox, T.; Caldwell, J. W.; Kollman, P. A. *J. Am. Chem. Soc.* **1995**, *117*, 5179–5197.

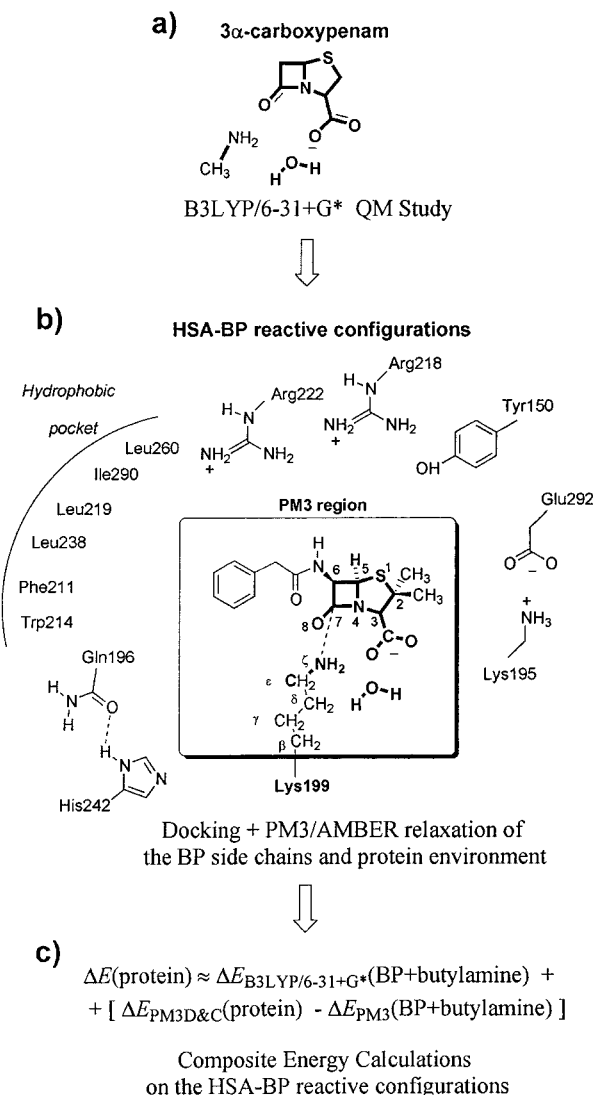


**Figure 2.** Schematic representation for the computational approach used in this work. (a) The internal geometry of the B3LYP/6-31+G\* TSs and intermediate for the water-assisted aminolysis of 3 $\alpha$ -carboxypenam (ref 18) was used to build the HSA-BP reactive configurations. (b) The critical points obtained for the 3 $\alpha$ -carboxypenam system were rigidly docked into the HSA-BP template whose construction is described in the text. The BP side chains as well as the surrounding water molecules and protein residues were relaxed by means of PM3/AMBER minimizations in the protein. The PM3 region and the most important HSA residues for BP binding are also indicated. Note that bonds in bold lines indicate the atoms subject to geometry constraints during the PM3/AMBER minimization. (c) Energy barriers were estimated by means of a composite procedure (see text for further details).

of the BP side chains and the surrounding protein residues and water molecules were allowed to relax via energy minimization (constraints were imposed on the reactive core to preserve its initial B3LYP/6-31+G\* geometry). Several configurations located along the B3LYP/6-31+G\* intrinsic reaction coordinate<sup>31</sup> (IRC) started at **TS<sub>C</sub>** for the CP + methylamine system were also docked into the HSA-BP template by constraining the internal geometry of the same atoms as in **TS<sub>C</sub>**. In the case of the tetrahedral intermediate (**I**) and the TS for proton transfer and  $\beta$ -lactam cleavage (**TS<sub>2</sub>**), the ancillary water molecule plays a passive role, and, therefore, its geometry was fully optimized during the PM3/AMBER minimizations of the corresponding HSA-BP structures.

(31) Fukui, K. *Acc. Chem. Res.* **1981**, *14*, 363–368.

Two different starting points were considered for the geometry optimization of a prereactive complex in the HSA protein (**C**). The first one was obtained from the reactant end of the IRC configurations of the water-assisted mechanism previously docked into the protein. This point was fully minimized using the PM3/AMBER method; that is, no constraints were imposed in the semiempirical part. Similarly, a reactant-like distorted configuration of the previously optimized **TS<sub>1</sub>** model was also fully minimized. Since the two minimized prereactive complexes between HSA and BP were very similar in their PM3/AMBER energies and in their geometries, only the structure derived from the IRC configuration is presented in this work. In a second stage, the PM3 internal geometry of the bicyclic skeleton of BP was replaced by that of 3 $\alpha$ -carboxypenam at the B3LYP/6-31+G\* level. This was followed by geometry optimization in which the internal geometry of the carboxypenam moiety was preserved in order to make the prereactive complex and the reactive configurations (i.e., **TS<sub>C</sub>**, **TS<sub>1</sub>**, etc.) structurally consistent. We note that the B3LYP/6-31+G\* prereactive complex for the CP + methylamine system in Figure 1 shows intermolecular contacts similar to those observed in the protein (see below), but it is different from that previously reported in ref 18. An analogous strategy was adopted to obtain the penicilloyl product structure in HSA, where the initial geometry for geometry optimization was derived from a product-like distorted configuration of **TS<sub>2</sub>** (the docking of the gas-phase B3LYP/6-31+G\* geometry required the rigid rotation of the C5–C6 and C6–C7 bonds).

PM3/AMBER geometry optimizations were carried out using the ROAR 2.0 program<sup>32</sup> without a nonbond cutoff and driven by a limited memory BFGS minimizer.<sup>33</sup> In the final optimized structures, the root-mean-square residual gradient was always less than 0.001 kcal/(mol Å).

**Composite Energy Calculations.** We used a composite procedure<sup>34</sup> which combines both B3LYP/6-31+G\* electronic energies and PM3 energies in order to estimate the energy profile of the water-assisted and carboxylate and water-assisted mechanisms in HSA. The coordinates of the PM3 region, including those of the hydrogen link atom, were extracted from the different PM3/AMBER minimized structures in the HSA model. Single-point B3LYP/6-31+G\* and standard PM3 calculations were carried out on the reactive subsystems which represent the water-assisted aminolysis reaction between BP and *n*-butylamine (BP + butylamine system). Linear scaling PM3 calculations were also performed on all of the HSA-BP structures using the “divide and conquer” (D&C) approach.<sup>35</sup> The various energies were then combined to estimate the relative energies of the critical structures in the HSA protein,  $\Delta E(\text{protein})$ , with respect to the prereactive complex using the following equation:

$$\Delta E(\text{protein}) \approx \Delta E_{\text{B3LYP/6-31+G}^*}(\text{BP} + \text{butylamine}) + [\Delta E_{\text{PM3D\&C}}(\text{protein}) - \Delta E_{\text{PM3}}(\text{BP} + \text{butylamine})] \quad (1)$$

where the second term in brackets is a semiempirical correction due to the effect of the protein environment and water on the energy barrier of the reactive subsystem computed at the higher level of theory.

We note that the main source of error in (1) will come from the electrostatic mismatches that arise along the reaction coordinate from the use of a semiempirical Hamiltonian to reproduce B3LYP/6-31+G\* charge density. To further analyze this, we determined the dipole moment, the electrostatic potential-derived atomic charges<sup>36</sup> (ESP), and

(32) Cheng, A.; Stanton, R. S.; Vincent, J. J.; van der Vaart, A.; Damodaran, K. V.; Dixon, S. L.; Hartsough, D.S.; Mori, M.; Best, S. A.; Monard, G.; Garcia, M.; Van Zant, L. C.; Merz, K. M., Jr., *ROAR 2.0*; The Pennsylvania State University, University Park, PA, 1999.

(33) Liu, D. C.; Nocedal, J. *Math. Program.* **1989**, *45*, 503–528.

(34) Raghavachari, K.; Curtiss, L. A. Evaluation of Bond Energies to Chemical Accuracy by Quantum Chemical Techniques. In *Modern Electronic Structure Theory Part II*; Yarkony, D. R., Ed.; World Scientific: Singapore, 1995.

(35) (a) Dixon, S. L.; Merz, K. M., Jr. *J. Chem. Phys.* **1996**, *104*, 6643–6649. (b) Dixon, S. L.; Merz, K. M., Jr. *J. Chem. Phys.* **1997**, *107*, 879–893. (c) van der Vaart, A.; Suárez, D.; Merz, K. M., Jr. *J. Chem. Phys.* **2000**, *113*, 10512–10523.

(36) Besler, B. H.; Merz, K. M., Jr.; Kollman, P. A. *J. Comput. Chem.* **1990**, *11*, 431–439.

the electrostatic free energy of solvation within a solvent continuum<sup>37</sup> at both the B3LYP/6-31+G\* and PM3 levels for all the structures in Figure 1. We found that the trends in the polarity of the structures are nearly identical at both levels. In general, the ESP charges of selected functional groups were found to be comparable. Nevertheless, the relative solute–solvent interaction energies ( $\Delta\Delta G_{\text{solv}}$  in Figure 1) give a more definitive measure of the environmental effects estimated semiempirically when compared with the B3LYP/6-31+G\* values. These solvation energies were obtained via a Poisson–Boltzmann method coupled with QM SCRF calculations where the solute is represented by a set of atomic charges and the solvent as a layer of charges at the solvent-exposed molecular surface.<sup>38,39</sup> We see that the PM3 and B3LYP/6-31+G\*  $\Delta\Delta G_{\text{solv}}$  terms for **TS<sub>C</sub>** are essentially identical (−18 kcal/mol), while the PM3 solvent effects along the carboxylate and water-assisted energy profile are underestimated (**TS<sub>1</sub>**, **I**) or overestimated (**TS<sub>2</sub>**) by about 2–4 kcal/mol. Other approximations implicit in eq 1, such as the inclusion of link atoms in the computation of the  $\Delta E_{\text{PM3}}$  and  $\Delta E_{\text{B3LYP/6-31+G*}}$  terms, may also have a minor influence. We observed that the quantum link atom charges are constant in the different structures, suggesting that these virtual H atoms would have a minimal effect on the results. Similarly, we found that the influence on energies by switching between the PM3 and B3LYP/6-31+G\* internal geometries for the ancillary water and/or the Lys199  $\epsilon$ -amino group was minimal (less than 1 kcal/mol).

Single-point B3LYP/6-31+G\* calculations<sup>40,41</sup> were carried out with the Gaussian98 suite of programs.<sup>42</sup> The DivCon99 program<sup>43</sup> was employed to perform the linear-scaling D&C PM3 calculations using the dual buffer layer scheme (inner buffer layer of 4.0 Å and an outer buffer layer of 2.0 Å) with one protein residue per core. A cutoff of 9.0 Å was used for the off-diagonal elements of the Fock, one-electron, and density matrixes. To test the stability and accuracy of the D&C PM3 relative energies, we also performed some D&C calculations using a second buffer strategy (inner buffer layer of 5.0 Å and outer buffer layer of 2.0 Å). Both D&C subsetting schemes with total buffer regions of 6.0 and 7.0 Å, respectively, gave relative energies that differed by less than 0.10 kcal/mol.<sup>35</sup>

The calculation of the electrostatic  $\Delta G_{\text{solv}}$  energies described above was done using the self-consistent reaction field method implemented in DivCon99<sup>43</sup> (PM3) and Jaguar<sup>44</sup> (B3LYP/6-31+G\*). All the reported atomic charges for the structures embedded in the HSA protein are charge-model 2 (CM2) charges<sup>45</sup> derived from gas-phase PM3 calculations on the QM region defined during minimization or obtained from D&C calculations on the entire HSA–BP protein system.

(37) Tomasi, J.; Persico, M. *Chem. Rev.* **1994**, *94*, 2027–2094.

(38) Gogonea, V.; Merz, K. M., Jr. *J. Phys. Chem. A* **1999**, *103*, 5171–5188.

(39) Tannor, D. J.; Marten, B.; Murphy, R.; Friesner, R. A.; Sitkoff, D.; Nicholls, A.; Ringnalda, M.; Goddard, W. A., III; Honig, B. *J. Am. Chem. Soc.* **1994**, *116*, 11875–11882.

(40) Becke, A. D. Exchange-Correlation Approximation in Density-Functional Theory. In *Modern Electronic Structure Theory Part II*; Yarkony, D. R., Ed.; World Scientific: Singapore, 1995.

(41) Hehre, W. J.; Radom, L.; Pople, J. A.; Schleyer, P. v. R. *Ab Initio Molecular Orbital Theory*; John Wiley & Sons Inc.: New York, 1986.

(42) Frisch, M. J.; Trucks, G. W.; Schlegel, H. B.; Scuseria, G. E.; Robb, M. A.; Cheeseman, J. R.; Zakrzewski, V. G.; Montgomery, J. A.; Stratmann, R. E., Jr.; Burant, J. C.; Dapprich, S.; Millam, J. M.; Daniels, A. D.; Kudin, K. N.; Strain, M. C.; Farkas, O.; Tomasi, J.; Barone, V.; Cossi, M.; Cammi, R.; Mennucci, B.; Pomelli, C.; Adamo, C.; Clifford, S.; Ochterski, J.; Petersson, G. A.; Ayala, P. Y.; Cui, Q.; Morokuma, K.; Malick, D. K.; Rabuck, A. D.; Raghavachari, K.; Foresman, J. B.; Cioslowski, J.; Ortiz, J. V.; Stefanov, B. B.; Liu, G.; Liashenko, A.; Piskorz, P.; Komaromi, I.; Gomperts, R.; Martin, R. L.; Fox, D. J.; Keith, T.; Al-Laham, M. A.; Peng, C. Y.; Nanayakkara, A.; Gonzalez, C.; Challacombe, M.; Gill, P. M. W.; Johnson, B.; Chen, W.; Wong, M. W.; Andres, J. L.; Gonzalez, C.; Head-Gordon, M.; Replogle, E. S.; Pople, J. A. *Gaussian 98*, Revision A.6; Gaussian, Inc.: Pittsburgh, PA, 1998.

(43) Dixon, S. L.; van der Vaart, A.; Gogonea, V.; Vincent, J. J.; Brothers, E. N.; Suárez, D.; Westerhoff, L. M.; Merz, K. M., Jr. *DIVCON99*; The Pennsylvania State University: University Park, PA, 1999.

(44) *JAGUAR 3.5*; Schrödinger, Inc.: Protland, OR, 1998.

(45) Li, J.; Cramer, C. J.; Truhlar, D. G. *J. Phys. Chem. A* **1998**, *102*, 1820–1831.

**Table 1.** Relative Energies (kcal/mol) of the Main Critical Structures Involved in the Water-Assisted Aminolysis Reaction of Benzylpenicillin

structure	$\Delta E_{\text{B3LYP/6-31+G*}}$		$[\Delta E_{\text{PM3D&C}}(\text{protein}) - \Delta E_{\text{PM3}}(\mathbf{B})]^a$	$\Delta E(\text{protein})^b$
	A CP + methylamine	B BP + butylamine		
<b>C</b>	0.0	0.0	0.0 (0.0)	0.0
<b>TS<sub>C</sub></b>	42.2	41.3	−3.4 (+21.2)	37.9
<b>TS<sub>1</sub></b>	28.7	26.2	+31.0 (+37.7)	57.2
<b>I</b>	21.2	32.3	+23.2 (+57.7)	55.5
<b>TS<sub>2</sub></b>	23.0	32.5	+20.1 (+35.2)	52.2
<b>P</b>	−27.2	−11.9	+5.7 (+20.0)	−6.2

<sup>a</sup>  $[\Delta E_{\text{PM3/AMBER}}(\text{protein}) - \Delta E_{\text{PM3}}(\mathbf{B})]$  values in parentheses.  
<sup>b</sup>  $\Delta E(\text{protein}) \approx \Delta E_{\text{B3LYP/6-31+G*}}(\mathbf{B}) + [\Delta E_{\text{PM3D&C}}(\text{protein}) - \Delta E_{\text{PM3}}(\mathbf{B})]$ .

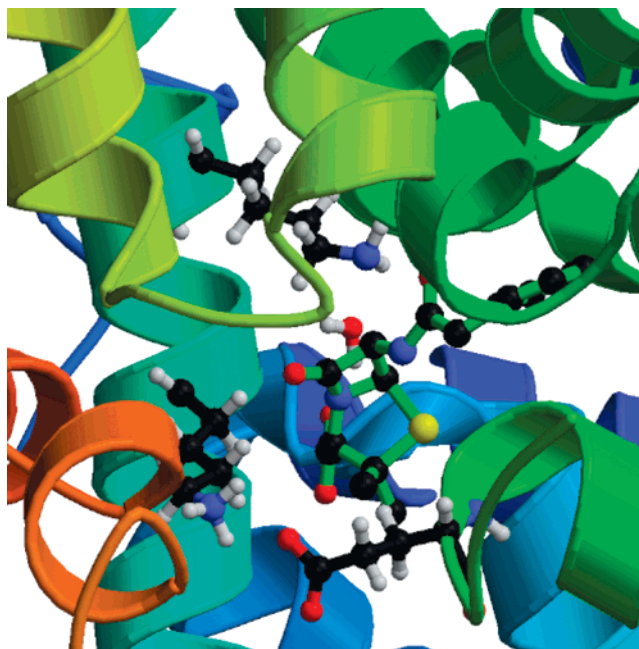


**Figure 3.** Ribbon model of the PM3/AMBER minimized structure of the prereactive complex for the aminolysis reaction of BP and Lys199 in the IIA binding site of HSA. Benzylpenicillin, the catalytic water molecule, and the side chains of Lys199, Lys195, and Glu292 are shown as ball-and-stick structures. This figure was produced with the programs Molscrip and Raster3D (refs 57 and 58).

## Results

Table 1 gives relative energies for the reactive configurations along the HSA–BP energy profiles. Figure 3 displays a view of the prereactive complex showing the most important protein–substrate contacts, which occur along the reaction profile. The QM region of the different structures as optimized with the PM3/AMBER method are shown in Figure 4, including the CM2 charges of selected functional groups. We note that the structure and properties of the TSs for the aminolysis reaction of model systems have been thoroughly discussed in previous work.<sup>15–19</sup>

**Prereactive Complex.** The PM3/AMBER minimized complex (**C**) shown in Figure 3 confirms that BP can bind noncovalently to the IIA binding site in an orientation where Lys199 can initiate the aminolysis reaction. The  $\epsilon$ -amino group of Lys199 establishes an  $\text{N}\cdots\text{H}-\text{C}$  hydrogen bond with the C6 position of BP which is also observed in the prereactive complex located in the gas phase (see Figure 1). The ancillary water molecule in **C** forms an H-bond with the  $\beta$ -lactam carboxylate group and an  $\text{O}\cdots\text{H}-\text{C}$  contact with the C5 atom of BP. The position of this water close to Lys199 is in agreement with the solvent structure observed in our previous MD study on the

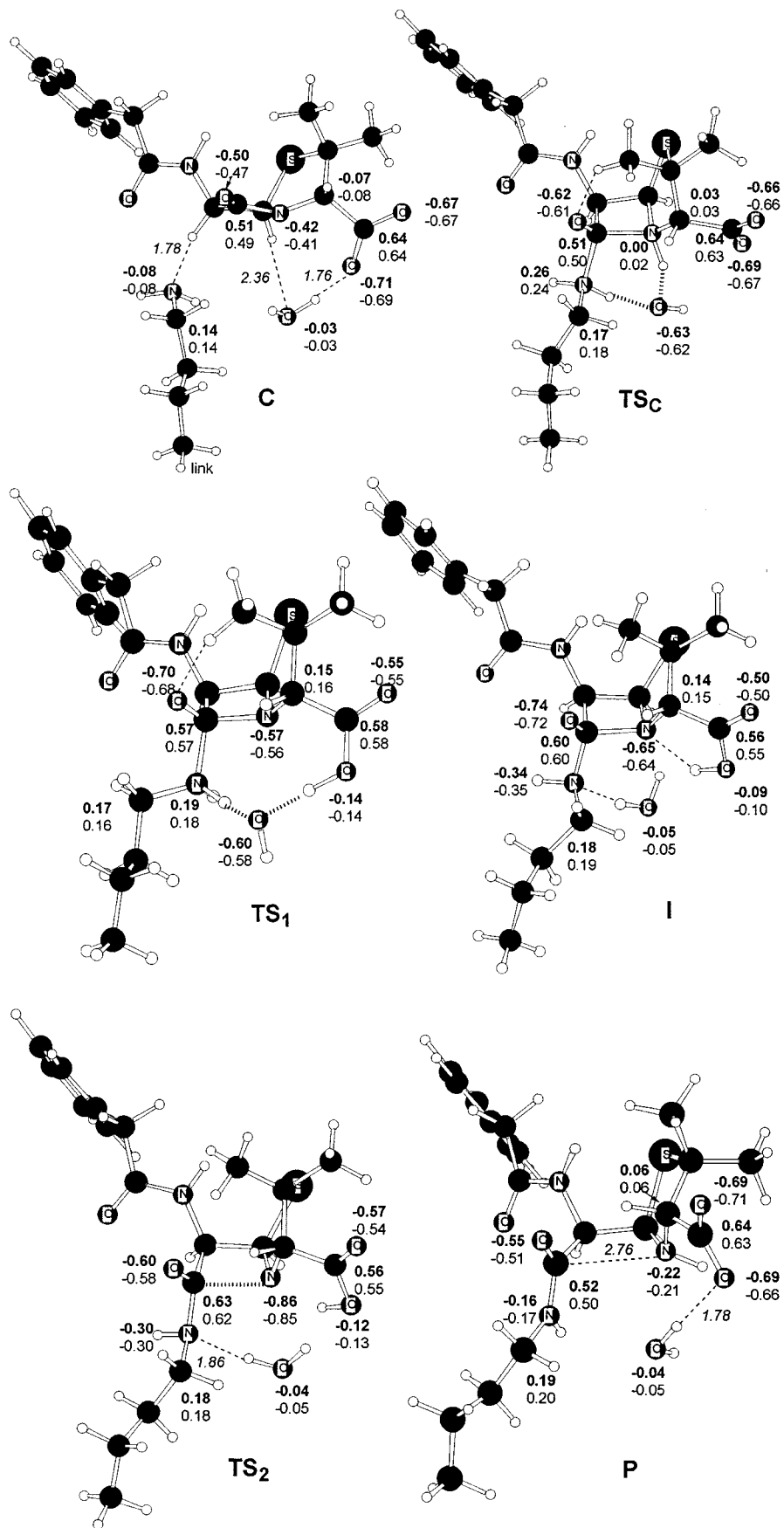


**Figure 4.** Optimized geometries of the QM region involved in the aminolysis reaction of BP in the HSA protein. Distances in Angstroms. Selected PM3 CM2 charges, with hydrogens summed into heavy atoms, are also indicated as calculated in the protein (bold figures) and in the isolated QM region.

**Table 2.** Relative Energies (kcal/mol) with Respect to the Prereactive Complex for Selected Structures along the IRC Path from **TS<sub>C</sub>** (*s* Stands for the Reaction Coordinate (amu<sup>1/2</sup> Bohr))

structure	C7–Nζ (Å)	C7–N4 (Å)	$\Delta E_{\text{B3LYP/6-31+G}^*}$		$[\Delta E_{\text{PM3D\&C}}(\text{protein}) - \Delta E_{\text{PM3}}(\mathbf{B})]$	$\Delta E(\text{protein})^a$
			A CP + methylamine	B BP + butylamine		
<i>s</i> = –1.64	1.78	1.54	32.1	33.9	–4.3	29.6
<i>s</i> = –0.68	1.70	1.62	38.2	38.7	–5.6	33.1
<i>s</i> = –0.48	1.69	1.63	40.4	41.4	–5.5	35.9
<i>s</i> = 0.0 ( <b>TS<sub>C</sub></b> )	1.66	1.65	42.2	41.3	–3.4	37.9
<i>s</i> = 0.72	1.58	1.74	39.5	40.2	–0.1	40.1
<i>s</i> = 0.84	1.56	1.76	38.0	39.9	–0.5	39.4
<i>s</i> = 1.10	1.53	1.80	33.2	35.2	2.1	37.3
<i>s</i> = 1.46	1.50	1.86	27.0	28.5	3.2	31.7

$$^a \Delta E(\text{protein}) \approx \Delta E_{\text{B3LYP/6-31+G}^*}(\mathbf{B}) + [\Delta E_{\text{PM3D\&C}}(\text{protein}) - \Delta E_{\text{PM3}}(\mathbf{B})].$$

native form of the IIA binding site.<sup>14</sup> Interestingly, the native residue–residue contacts in this region of the HSA binding pocket can be maintained in the protein–substrate complex.<sup>9,14</sup> For example, the Nζ@Lys195···Oδ@Glu292 salt bridge, which plays an important structural role in the hydrophilic entrance to the IIA binding site, is preserved as well as the Nδ1@His242···Oδ@Gln196 H-bond which connects the two polar residues adjacent to the nucleophilic Lys199.

Hydrophobic interactions are clearly an important determinant in penicillin binding to HSA because the aromatic side chain of BP is completely buried in the IIA hydrophobic pocket. For example, the side chains of Ile290, Leu219, Leu260, Val241, Leu238, Trp214, and Phe211 have contacts with the acylamino side chain of BP. Electrostatic interactions are also favorable in this mode of binding: the β-lactam carbonyl group, which is oriented toward the side chains of Arg218 and Arg222, is capped by a cluster of water molecules at the entrance of the IIA binding site, while the penicillin carboxylate group is near the Lys195–Glu292 salt bridge. Although this carboxylate group is normally considered to enhance enzyme–substrate binding through the formation of salt bridge contacts with protonated lysine or arginine residues in the active site of β-lactam-recognizing enzymes,<sup>46</sup> this group is partially desolvated and does not establish any specific salt bridge interaction in our model of the IIA binding site.

Globally, the nature of the HSA–BP interactions present in **C** is in good agreement with experimental data, showing that HSA and penicillins form relatively weak complexes stabilized by both electrostatic interactions and hydrophobic effects with  $\Delta G_{\text{binding}} \approx +5, +6$  kcal/mol.<sup>7,47</sup> The experimental thermodynamic parameters for various penicillin–albumin complexes suggest that penicillins do not form hydrogen bonds with albumin due to the slightly endothermic nature of the binding process ( $\Delta H_{\text{binding}} \approx 1$  kcal/mol).<sup>47</sup> This agrees with the structure of the prereactive complex in Figure 3, which does not establish clear H-bond contacts with the surrounding residues except the C–H···N contact with Lys199. We also note that the absence of a salt bridge between HSA and the penicillin carboxylate group could explain the weak binding character of this complex.

We expected that the HSA protein would not undergo significant changes in structure on conversion from the prereactive complex to the transition structures.<sup>48</sup> In agreement with this, we observed that the protein–substrate contacts, for the remainder of the structures docked into HSA, were nearly identical to those observed in **C**. Indeed, the RMS deviations

of the protein atoms were always lower than 0.10 Å with respect to **C**. Therefore, we conclude that **C** is a good representative of a near attack conformer<sup>48</sup> from which the relative energy barriers in the protein can be computed. Thus, the resulting energy differences reflect the inherent stability of the reactive region (i.e., BP, the Lys199 side chain and the ancillary water molecule) and its interaction with the protein environment.

**Concerted Water-Assisted Mechanism.** In the concerted aminolysis process, the water molecule catalyzes the H-transfer from the nucleophilic amino group of Lys199 to the N4 atom in the β-lactam ring with simultaneous bond fission of the endocyclic C7–N4 bond. In the structure of the corresponding **TS<sub>C</sub>**, the catalytic water molecule shows a hydroxide character while the carbonyl group accumulates a negative charge of ~0.10e with respect to the prereactive complex. The amine moiety, which has not yet transferred the proton (N–H distance ~1.1 Å), has a positive charge of ~0.25 e (see the CM2 charges in Figure 4). The model of the concerted **TS** for the reaction between HSA and BP gives a  $\Delta E(\text{protein})$  energy barrier of 37.9 kcal/mol, while the  $\Delta E_{\text{B3LYP/6-31+G}^*}$  barrier of the CP + methylamine system and that of the related BP + butylamine model systems have values of 42.2 and 41.3 kcal/mol, respectively. Thus, we see that the influence of substituents and the protein is moderate in this case. The weak effect of substituents can be understood in terms of the electron-withdrawing ability of the acylamino side chain which can stabilize the partial negative charge of the carbonyl group.

To discuss the possible structural effects of the protein environment on the concerted mechanism, we present in Table 2 some geometric and energetic data corresponding to selected structures along the IRC path from **TS<sub>C</sub>** (originally calculated for the CP + methylamine system in the gas phase). By comparing the relative energies of the BP + butylamine model in the gas phase and in the protein with those of the unsubstituted system, the structural invariance of the main **TSs** for the aminolysis of β-lactams can be quantitatively assessed. As expected, substitution has only a minor effect on the relative energies so that the location of the structure with the maximum energy remains essentially unaltered (see Table 2). On the other hand, the protein effects moderately stabilize the reactant-like configurations adjacent to **TS<sub>C</sub>** and seem to destabilize the product-like ones. As a consequence, the maximum energy point along the reaction profile embedded in the HSA protein is slightly shifted toward products (reaction coordinate *s* = +0.72). We note, however, that the energetic and structural features of this “shifted” point and those of the **TS<sub>C</sub>** structure are similar. Their relative energies in the protein differ by only 2.2 kcal/mol and their reactive bond distances by ±0.10 Å. Hence, we conclude that the geometric and energetic consequences of the protein effects are small in this class of **TSs**.

(46) Waley, S. G. β-lactamase: mechanism of action. In *The Chemistry of β-lactams*; Page, M. I., Ed.; Blackie Academic & Professional, London, 1992; pp 199–228.

(47) Landau, M. *Russ. J. Org. Chem.* **1998**, *34*, 615–628.

(48) Bruice, T. C.; Benkovic, S. J. *Biochemistry* **2000**, *39*, 6267–6274.

**Carboxylate and Water-Assisted Mechanism.** In our previous work on the gas-phase model systems,<sup>18</sup> it was shown that the penicillin carboxylate group may shuttle the proton required to form and, subsequently, cleave the tetrahedral intermediate. This mechanism proceeds initially through a TS, **TS<sub>1</sub>**, in which the nucleophilic attack of the Lys199  $\epsilon$ -amino group takes place with simultaneous H-transfer to the carboxylate group assisted by an ancillary water molecule. At **TS<sub>1</sub>** the forming C7–N $\zeta$  bond is quite “late”, and the catalytic water molecule moiety has hydroxide character as in the **TS<sub>C</sub>** structure (see Figure 4). However, the partitioning of the computed energy barrier in the protein for **TS<sub>1</sub>** (57.2 kcal/mol) into contributions for the reactive subsystem (26.2 kcal/mol) and the protein effect term (31.0 kcal/mol) indicate that this carboxylate and water-assisted process is strongly destabilized by the protein environment (see below).

**TS<sub>1</sub>** is connected to the amino-alcoholate tetrahedral intermediate **I** in which the C7–N4 bond is clearly weakened while the hydroxyl group of the carboxylic acid establishes an H-bond with the N4 atom, which is suitably oriented for proton transfer. The ancillary water molecule, which is fully relaxed during the PM3/AMBER minimization within the protein, is positioned below the  $\beta$ -lactam ring, solvating the exocyclic amino group via a typical H-bond as in the corresponding B3LYP/6-31+G\* gas-phase structure of the CP + methylamine model system. The rupture of the tetrahedral intermediate can be generated via **TS<sub>2</sub>** in which the endocyclic C7–N4 bond is almost broken ( $\sim 2.0$  Å), whereas the proton shift from the carboxylic group to the forming amino group is in its initial stages.

We see in Figure 4 that the N $\zeta$ , N4, and the O8 atoms in **I** and **TS<sub>2</sub>** accumulate the major part of the global negative charge. The  $\Delta E_{\text{B3LYP/6-31+G}^*}$  terms for the BP + butylamine system reveal that the **TS<sub>2</sub>** structure is  $\sim 6$  kcal/mol above **TS<sub>1</sub>**, while **TS<sub>2</sub>** is  $\sim 6$  kcal/mol more stable than **TS<sub>1</sub>** for the CP + methylamine energy profile (see Table 1). This is most probably related to the electron-withdrawing effect of the acylamino side chain so that the partial zwitterionic C7–N4 bond becomes more destabilized in **I** and **TS<sub>2</sub>** than the amidic C7–N4 bond at the initial stages of the reaction. However, inclusion of protein effects compensates the influence of substituents, and the **TS<sub>1</sub>**, **I**, and **TS<sub>2</sub>** structures docked in the HSA protein have  $\Delta E(\text{protein})$  values of 57.2, 55.5, and 52.2 kcal/mol, respectively. These figures indicate that the existence of intermediate species along the carboxylate and water-assisted mechanism would be only transient. Most importantly, the magnitude of the rate-determining energy barrier in the IIA binding site predicts that this mechanism becomes clearly disfavored by  $\sim 20$  kcal/mol with respect to the concerted water-assisted mechanism.

**Product Complex.** The structure of a penicilloyl product complex obtained from the PM3/AMBER minimizations is shown in Figure 4. In the protein, the estimated reaction is exoergic by  $-6.2$  kcal/mol. The reaction energy for the BP + butylamine subsystem is  $-11.9$  kcal/mol, while the corresponding value for the CP + methylamine model is  $-27.2$  kcal/mol. These values seem to indicate that both substitution effects and protein effects might disfavor the thermodynamics of the process. We note, however, that the product complex in the protein has a short nonbonding C7 $\cdots$ N4 contact of 2.76 Å as a consequence of the sterically hindered conformation of the C5–C6 and C6–C7 bonds (see Figures 2 and 4). This is due to the fact that the protein environment in our HSA model, which is more adapted to the prereactive complex and TSs, limits the conformational space of the product complex. Therefore, a further relaxation by means of MD simulations might be

necessary in order to explore in detail the energetics and structure of the ground-state conformer of the HSA–penicilloyl conjugate.

**Protein Effects.** As mentioned in the Introduction, the IIA binding site of HSA can accommodate a broad class of hydrophobic organic anions of medium size which interact with HSA through a combination of electrostatic and hydrophobic forces.<sup>7</sup> For the critical structures in the aminolysis of BP embedded in the HSA model, the position of the lipophilic chain of BP hardly varies, and, therefore, the influence of hydrophobic HSA-BP interactions along the energy profile should be minimal. In contrast, the charge distribution changes quite dramatically in the reactive configurations owing to the highly polar character of the main TSs and the possible kinetic role (proton transfer group) of the penicillin carboxylate group. Thus, the relative protein effect energies of the TSs and intermediate with respect to the prereactive complex should be mainly determined by electrostatics.<sup>49</sup>

To estimate the polarization effects on the critical point structures due to HSA, we computed the PM3 CM2 atomic charges of the reactive atoms both in the protein (via PM3 D&C) and in the gas phase (see Figure 4). In general, we found that changes at the mechanistically important atoms were quite moderate ( $\pm 0.02$  e) and that the charge separations of the most polar bonds (e.g., the carbonyl group at C7) were slightly increased in the protein. However, the nature and magnitude of these variations are not directly correlated with the actual energetic impact of the protein environment. Thus, according to the  $\Delta E_{\text{PM3D\&C}} - \Delta E_{\text{PM3}}$  values collected in Table 1, the water-assisted mechanism in the protein is slightly favored by  $\sim 3$  kcal/mol, while the carboxylate and water-assisted mechanism is strongly destabilized up to 31 kcal/mol in the case of **TS<sub>1</sub>**. At **TS<sub>C</sub>**, the penicillin carboxylate group plays a passive role, and its interaction with the protein environment is very similar to that of the prereactive complex. Since the carbonyl oxygen atom in **TS<sub>C</sub>** is partially oriented toward Arg218 and Arg222 ( $\text{O}\cdots\text{N}\epsilon@ \text{Arg218} = 7.7$  Å,  $\text{O}\cdots\text{N}\epsilon@ \text{Arg222} = 6.5$  Å), the increase of the partial negative charge ( $-0.10$  e) on the carbonyl group could be stabilized (via analogy with the oxyanion hole concept in serine proteases) by these positively charged residues.

In the carboxylate and water-assisted mechanism, the carboxylate group plays an active role by accepting a proton from the Lys199 amino group and donating it to the endocyclic N4 atom of BP. From the geometry and charge distribution of **TS<sub>1</sub>**, **I**, and **TS<sub>2</sub>**, we see that the carboxylate group is effectively neutralized in these critical structures. In previous work,<sup>18</sup> we have speculated that the carboxylate and water-assisted mechanism, which is more favorable than the water-assisted route in the gas phase, could be favored owing to the presence of the hydrophobic pocket near the Lys199 residue which defines a low-polarity local region. Nevertheless, our present calculations demonstrate that the delocalization of the global negative charge of BP throughout the reactive atoms in the transition structures and intermediate influences the HSA–BP electrostatic interactions. The large impact on the **TS<sub>1</sub>** structure can be understood in terms of the delocalization of the negative charge through the N $\zeta$ H $\cdots$ OH $\cdots$ HO bridge connecting the amino and carboxylate groups, which affects the protein–substrate electrostatic interactions. In the second part of the carboxylate and water-assisted mechanism, the global negative charge of **I** and **TS<sub>2</sub>** is more concentrated on the N $\zeta$  and N4 atoms, and these structures are predicted to be less destabilized than **TS<sub>1</sub>**. Thus, while it

(49) Warshel, A. *Computer Modeling of Chemical Reactions in Enzymes and Solutions*; John Wiley & Sons: New York, 1991.



has been speculated that the charge delocalization in the stepwise mechanism would accelerate the reaction in the HSA protein due to the presence of the hydrophobic pocket, it is clear that this is not the case. Alternative longer range interactions appear to stabilize the localization of the negative charge in the water-assisted mechanism, thereby favoring it in HSA.

At this point it is interesting to note that, in the context of the structure and function of HSA, the protein–substrate reaction between Lys199 and BP would be best considered as a secondary aspect of the noncovalent drug binding processes that occur in the IIA binding site. Our calculations on the magnitude of the energy barrier in the protein support this view by suggesting that HSA shows little to no catalytic activity in the aminolysis reaction of BP. This is not a surprising conclusion given that HSA is a small molecule binding protein and not a catalytic system per se.

**Comparison between the PM3 D&C and PM3/AMBER Energies.** It is well known that the application of QM/MM methodologies to the study of the energetics of reaction mechanisms in enzymes has some unresolved problems: where to assign the QM/MM boundary, how to treat the chemical bonds crossing the two regions, the neglect of charge polarization of the MM region in most of the QM/MM methods, etc.<sup>50</sup> These issues do not arise when the entire system is treated quantum mechanically as in PM3 D&C calculations. Therefore, it is interesting to compare the protein effects predicted by the PM3/AMBER Hamiltonian with those obtained using the linear-scaling D&C PM3 method. To this end, the corresponding  $\Delta E_{\text{PM3/AMBER}} - \Delta E_{\text{PM3}}$  terms for the different critical points are also included in Table 1.

In general, we see in Table 1 that the  $\Delta E_{\text{PM3/AMBER}} - \Delta E_{\text{PM3}}$  terms measuring the protein effects predict an energy profile in the protein that is less stable (by about 7–34 kcal/mol) than that obtained from the PM3 D&C calculations. The QM/MM methodological problems could be responsible for this discrepancy between the PM3/AMBER and PM3 D&C energies. We believe that the division between a *hard* set of point charges representing the MM region and a *soft* QM charge density yields an unbalanced description of the changes in the protein–substrate interactions when electronic differences arise along a reaction profile like that of the aminolysis of BP.

## Discussion

**Comparison with Kinetic Data on the Penicillin Haptenation to HSA.** To find out if our results are consistent with the basic chemical events which take place during the conjugation of penicillins to serum albumin, the magnitudes of the computed energy barriers for the different models were compared with experimental data on the haptenation kinetics. According to the energy profiles in Table 1, the water-assisted concerted mechanism for the formation of the amide linkage between BP and Lys199 is the most favorable one, with an energy barrier of  $\sim 38$  kcal/mol with respect to the prereactive complex. In terms of free energies, it is reasonable to expect that the actual barrier in the protein would be lower due to entropic contributions arising from the structural elasticity of the protein environment, but these effects were not considered here. Nevertheless, it is also clear that the theoretical value of the energy barrier ( $\sim 38$  kcal/mol) is not compatible with fast kinetics.

Recently, the kinetics of [<sup>3</sup>H]benzylpenicillin conjugation to excess of HSA at pH 7.3–7.4 has been followed by means of

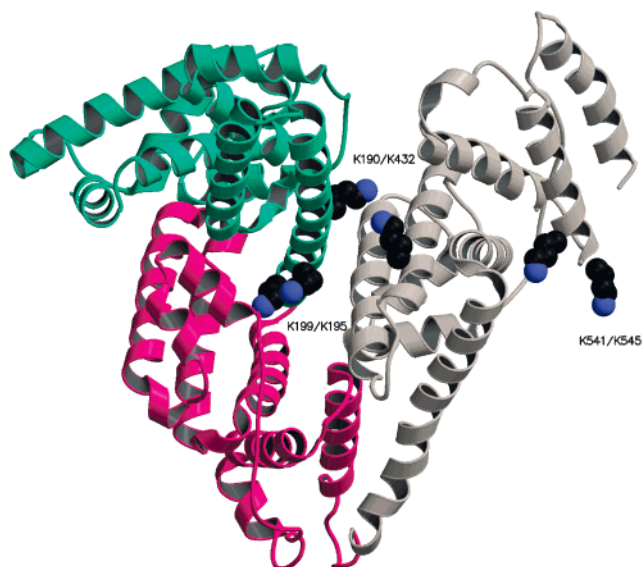


**Figure 5.** Ribbon model of HSA derived from X-ray crystallography. The penicillin-binding lysine residues are represented by van der Waals spheres. This figure was produced with the programs Molscript and Raster3D (refs 57 and 58).

a liquid scintillation counting method in 1–2 mL of [<sup>3</sup>H]-BP solution with an activity of 44 000 disintegrations per minute.<sup>51</sup> The sensitivity of these experiments allowed the formation of the HSA–penicilloyl conjugates to be readily monitored at 37 °C. Over the first 24 h, an average rate of 66 detected counts per minute was measured. This low activity for the formation of HSA–penicilloyl conjugates corresponds to  $\sim 3.5\%$  of the initial BP fixed to HSA after 24 h of reaction. Although radiation detectors can detect only a fraction of the  $\beta$  emissions, it is clear that the aminolysis reaction between HSA and BP follows extremely slow nonenzymatic kinetics. Similar observations were also reported in the 1960s for the reactions of BP with HSA<sup>52</sup> and polylysine,<sup>53</sup> although activation parameters for these processes have not been reported. Interestingly, it has been shown that the direct reaction of BP with *n*-butylamine in aqueous solutions at pH 7.4 is also very slow, with an expected half-life of  $\sim 100$ –400 h.<sup>54</sup> Overall, the experimental evidences, though not directly comparable with theory, correlate well with the predicted high energy barrier for the aminolysis reaction between BP and the Lys199 residue in HSA.

**Chemical Reactivity of Other Lysine Residues.** Although the primary site of penicilloyl coupling is the  $\epsilon$ -amino group of Lys199, penicilloyl groups have been also detected experimentally on other lysine residues of HSA (Lys190, Lys195, Lys432, Lys541, and Lys545).<sup>10</sup> Interestingly, Lys195 is near Lys199 in the IIA binding site, suggesting that the combination of two closely located  $\epsilon$ -amino groups could have possible structural and/or mechanistic consequences. Furthermore, the X-ray structure of HSA<sup>9</sup> has also revealed that the pairing of lysine residues is also a major feature of the structure of the other penicillin binding sites (see Lys190/Lys432 and Lys541/Lys545 in Figure 5). This structural pairing of the reactive lysine groups is consistent with the experimental observation that there are

(51) DiPiro, J. T.; Adkinson, N. F.; Hamilton, R. G. *Antimicrob. Agents Chemother.* **1993**, *37*, 1463–1467.

(52) Batchelor, F. R.; Dewdney, J. M.; Gazzard, D. *Nature* **1965**, *206*, 362–364.

(53) Schneider, C. H.; de Weck, A. L. *Nature* **1965**, *208*, 57–59.

(54) Yamana, T.; Tsuji, A.; Miyamoto, E.; Kiya, E. *J. Pharm. Pharmacol.* **1975**, *27*, 56–58.

(50) Titmuss, S. J.; Cummins, P. L.; Bliznyuk, A. A.; Rendell, A. P.; Gready, J. E. *Chem. Phys. Lett.* **2000**, *320*, 169–176.

never more than two or three penicillin molecules bound to a single HSA molecule.<sup>55</sup>

In the case of the IIA binding site, MD simulations have shown that the most likely configuration for the Lys195/Lys199 pair corresponds to the neutral  $\epsilon$ -amino group of Lys199 connected to the acid form of Lys195 through a network of H-bonding water molecules.<sup>14</sup> We have proposed that this acid–base pair could undergo proton interchange easily and, consequently, both lysine residues could have an enhanced nucleophilic ability, as experimentally observed in the case of penicillin binding to HSA.<sup>10</sup> We note that similar considerations could apply to the other two penicillin binding sites; that is, it may be that each pair of lysine residues constitutes an acid–base pair subject to water-assisted proton interchange so that the lone pair of the neutral amino group could be a more effective nucleophile against penicillins.

**A Global View on Penicillin Haptenation to HSA.** Knowledge regarding the structure and properties of HSA can be combined with our theoretical results to obtain a more general view of the chemical reactions between HSA and penicillins. First, we note that the absence of sophisticated catalytic machinery in the HSA molecule is consistent with the existence of multiple reactive amino groups to penicillin. Indeed, the proposed mechanism of action is similar to that found in aqueous solution for the reaction of amines and CP, where a “bulk” water molecule plays an important catalytic role in the nonassisted process.<sup>18</sup> Lys199 reacts with penicillins because of its neutral character and its location in the IIA binding site, which has a high “noncovalent” affinity for hydrophobic organic anions such as BP (i.e., this is a proximity or entropic effect). The water molecule necessary to assist the reaction can be provided by the bridge of water molecules connecting the Lys195 and Lys199 residues in the IIA binding site. We also propose that one of the reactive amino groups in the other reactive pairs (e.g., Lys541/Lys545) should be deprotonated in order to become an efficient nucleophile.

**Specificity of Penicillin Antibodies.** As mentioned in the Introduction, extensive immunochemical studies have demonstrated that most of the penicillin antibody response is directed against the penicilloyl groups conjugated to HSA.<sup>1–3</sup> Initially, it was thought that the core of the penicillins (the degraded  $\beta$ -lactam-thiazolidine region) was the most important part of the antigenic determinant structure and that the acylamino side chain played only a minor role in the specificity of the antibody produced. However, a more complex pattern of antibody specificity has emerged in which at least two populations of penicillin-reacting antibodies appear to be present in the human sera. One recognizes the common structural motif (i.e., the bicyclic skeleton), and the other discriminates among different acylamino side chains as antigenic determinants.<sup>1</sup> In addition, the specific antibodies directed toward penicillins can recognize other  $\beta$ -lactam antibiotics (cross-reactions), though often with a lower efficiency. In this case, it is normally assumed that the most abundant *nuclear* antibodies induced by the penicillin–HSA conjugates recognize the degraded bicyclic part of a broad range of antibiotics, thereby explaining the cross-reactivity

observed between penicillins and the structurally related cephalosporins.<sup>2,3</sup> In contrast, the side-chain specificity of penicillin-induced antibodies is normally associated with low potential cross-reaction ability, which affects only those  $\beta$ -lactam antibiotics with the same or very similar side chains regardless of their class-defining core.

Herein, we speculate on the fact that the surface accessibility of the HSA–BP conjugates might determine the immune response in the form of *nuclear* antibodies (requires an accessibility to the thiazolidine moiety) and *side-chain* antibodies (requires accessibility to the side chain of the penicilloyl group). In our hypothesis, the location of the reactive lysine residues as well as the characterization of the mode of binding of penicillins could provide some insight into the origin of the specificity and cross-reactivity of penicillin antibodies. The Lys195 and Lys199 residues are situated at the entrance of the IIA binding site and have solvent-accessible surface areas<sup>56</sup> (SASA) of 49.5 and 4.0 Å<sup>2</sup>, respectively, in the X-ray structure. According to our modeling of the HSA–BP reaction, the acylamino side chain of the penicilloyl group linked to Lys199 would be deeply buried in the hydrophobic pocket, whereas the degraded  $\beta$ -lactam-thiazolidine nucleus would be partially solvent accessible with calculated SASA values of  $\sim 20$  Å<sup>2</sup>. A similar pattern could well occur for penicilloyl groups bound to Lys195, and, therefore, we propose that penicilloyl groups formed in the IIA binding site would stimulate the formation of *nuclear*-specific antibodies. In contrast, there are no hydrophobic pockets close to the other penicillin binding sites, and the SASA values for Lys190 (18.6 Å<sup>2</sup>), Lys432 (54.1 Å<sup>2</sup>), Lys541 (140.8 Å<sup>2</sup>), and Lys545 (110.1 Å<sup>2</sup>) indicate significant exposure to solvent (especially for the Lys541/Lys545 pair). It is conceivable that these lysine residues would yield penicilloyl groups with well-exposed side chains that would be responsible for eliciting the formation of *side-chain*-specific antibodies against penicillins.

## Summary

The calculated energy profile for the aminolysis reaction in the IIA subdomain of the HSA protein between the  $\epsilon$ -amino group of Lys199 and benzylpenicillin predicts that penicillin haptenation to HSA proceeds through a water-assisted one-step mechanism, which has a high energy barrier ( $\sim 38$  kcal/mol), in agreement with available experimental evidence. Taking into account both the tertiary structure of HSA and the mechanistic details, these results could increase our understanding of the origin of the specificity of antibodies and the cross-reaction processes between different classes of  $\beta$ -lactam antibiotics, which are characteristic of the immunochemistry of penicillins.

**Acknowledgment.** We thank the NIH for support of this work via grant GM44974. We also thank the National Center for Supercomputer Applications (NCSA) for generous allocations of supercomputer time. N.D., D.S., and T.L.S. are grateful to MCyT (Spain) for partial financial support (PB97-1300). N. D. thanks MCyT for Grant PB98-44430549.

JA010332J

(56) Connolly, M. L. *J. Appl. Crystallogr.* **1983**, *16*, 548–558.

(57) Kraulis, P. J. *J. Appl. Crystallogr.* **1991**, *24*, 946–950.

(58) Merritt, E. A.; Bacon, D. J. *Methods Enzymol.* **1997**, *277*, 505–524.

(55) Fischer, J. J.; Jardeztky, O. *J. Am. Chem. Soc.* **1965**, *87*, 3237–3245.